ELSEVIER
Available online at www.sciencedirect.com
ScienceDirect
Mendeleev Commun., 2020, **30**, 663–665
Mendeleev Communications

Electrochemical dispersion technique for the preparation of Sn-doped Pt particles and their use as electrocatalysts

Alexandra B. Kuriganova,*[a] Igor N. Leontyev,[b] Anna A. Ulyankina[a] and Nina V. Smirnova[a]

[a] *Platov South-Russian State Polytechnic University, 346428 Novocherkassk, Russian Federation. E-mail: kuriganova_@mail.ru*
[b] *Southern Federal University, 344006 Rostov-on-Don, Russian Federation*

DOI: 10.1016/j.mencom.2020.09.037

The Pt nanoparticles doped with tin were prepared by an electrochemical dispersion pulse alternating current technique, and their enhanced catalytic activity in the electrochemical oxidation of ethanol was estimated.

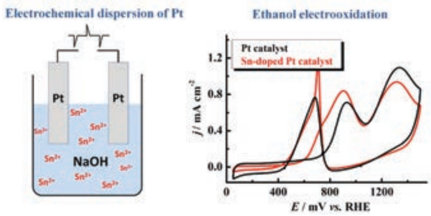

Keywords: tin, platinum, electrochemical dispersion, alternating current, ethanol electrooxidation, fuel cell, electrocatalysis.

Metal doping/alloying strategies for the synthesis of bi- or polymetallic nanoparticles (NPs)[1,2] are of great current interest due to their potential applications to fuel cell technologies,[1,3–5] lithium-ion batteries,[6] photocatalysis,[7,8] *etc*.[9,10] In the development of metal alloy nanocatalysts, in particular, platinum-based alloys, considerable attention has been paid to the composition-, size- and structure-controlled synthesis of catalytically active NPs to improve their catalytic selectivity and activity.[2,11,12] Unfortunately, a large number of metals cannot readily form alloys not only under ambient conditions but also over wide temperature ranges. Therefore, the high-temperature processing of two bulk metals is conventionally required for the synthesis of bimetallic alloys.

Moreover, bimetallic NPs can be produced by laser ablation,[13,14] induction melting[15] as well as microwave[16] and electrochemical[17,18] syntheses. Typically, the production of nanoparticles at elevated temperatures (>600 °C) leads to their sintering and increasing the size. Platinum-based materials including tin as adatoms[19] and platinum–tin alloys[20] or oxide composites[21] are well known as promising catalysts for the electrochemical oxidation of ethanol in the development of direct alcohol fuel cells. It was found that the catalytic activity of Pt-based materials in electrooxidation processes increased considerably upon doping metal oxide supports with tin.[22,23] However, data on the tin-doped Pt nanoparticles are scanty.[24] As we reported earlier, the catalytic materials based on platinum,[25] Pt_xNi nanoparticles[26] and $Pt_{90}Ir_{10}$[27] alloys can be easily synthesized by the electrochemical dispersion of metal foil (Pt, Pt_3Ni or $Pt_{90}Ir_{10}$) under alternating pulse current in an alkaline electrolyte. Electrolyte components can be introduced into the particles formed *via* metal electrode dispersion.[21,28] In this work, we modified the electrochemical dispersion pulse alternating current technique (EDPAC) to obtain $PtSn_x$ NPs by means of electrochemical dispersion of Pt electrodes in a tin-containing electrolyte.

In the EDPAC synthesis[†] of electrocatalysts in a 2 M aqueous NaOH solution in the absence or presence of tin ions, intense dispersion of platinum electrodes in the electrolyte was observed.[25,27] The calculated rate of platinum dispersion (V_{disp}) was 11 ± 1 mg cm^{-2} h^{-1} regardless of the presence of tin ions in the NaOH solution. Moreover, the applied average current density had only a very slight effect on V_{disp} of platinum electrodes in both electrolytes. Figure 1 shows a maximum of V_{disp} at j = 1.0 A cm^{-2}.

Figure 2 shows the X-ray diffraction pattern[‡] of the $PtSn_x$ sample with two sets of diffraction peaks. The first set contains

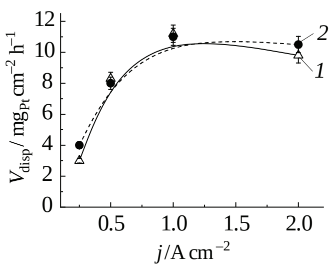

Figure 1 Dependence of the Pt dispersion rate on the electrolyte composition and current density: *(1)* 2 M NaOH + 1 M $SnSO_4$ and *(2)* 2 M NaOH.

[†] The $PtSn_x$/C electrocatalysts were obtained by the EDPAC technique as described previously.[25] Two Pt foil electrodes were immersed in an aqueous suspension (90 ml of 2 M NaOH + 10 ml of 1 M $SnSO_4$) and electrochemically dispersed under a pulsed ac operation at 50 Hz; the current density was 1 A cm$^{-2}_{geom}$. Finally, the freshly prepared $PtSn_x$/C electrocatalyst was filtered off, washed with distilled water and dried at 80 °C. Carbon support (Vulcan XC-72) was added to the final $PtSn_x$ particles during a ‘catalytic ink’ mixing procedure. The content $PtSn_x$ of the final catalyst was at least 20%. For comparison, a Pt/C catalyst was synthesized according to a similar procedure.[25]

[‡] The XRD analysis was performed on an ARL X’TRA powder diffractometer, Thermo Scientific, (CuKα, 1.5418 Å). XRD data were collected in a 2θ range of 20–90° using the step scan mode with a step width of 0.01° and a step time of 2.00 s.

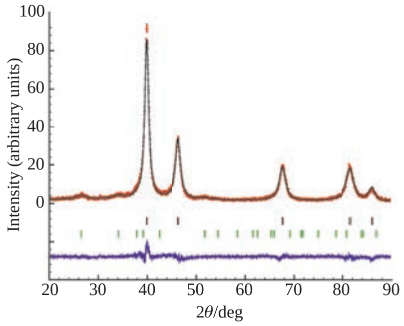

Figure 2 X-ray diffraction pattern of $PtSn_x$ synthesized under unsteady electrolysis conditions (red points, observed intensity; black solid line, intensity calculated by the Rietveld method; blue line, difference between the observed and calculated intensities; black and green tick marks correspond to fcc structures of platinum and SnO_2 phases, respectively).

the high-intensity broadened characteristic peaks of a face-centered Pt cell with the *Fm*3*m* space group. The second set corresponds to the widened peaks of a tetragonal phase of SnO_2 with the space group *P*42/*mnm*. The Rietveld refinement was carried out for two phases simultaneously using the spherical harmonics method for two sets for point groups *m*3*m* and 4/*mmm* to determine the average size of nanoparticles and microstresses. The resulting $PtSn_x$ NPs have a unit cell parameter $a = 3.9174 \pm 0.0004$ Å. The NPs size averaged over all crystallographic directions and average maximum strain are 5.6 ± 0.6 and $23 \pm 4 \times 10^{-4}$ nm, respectively. In this case, the unit cell parameter of the synthesized $PtSn_x$ NPs is higher than that of Pt NPs ($a = 3.9131$ Å) by 0.0043 Å.[29] The expansion of a Pt lattice may be attributed to the tin doping of Pt NPs. According to the refinement results, the concentration of tin oxide nanoparticles is 11% with respect to Pt and $PtSn_x$.

Figure 3 shows an image of the synthesized $PtSn_x$ sample obtained by scanning transmission electron microscopy (STEM)[§]. It can be seen that Pt and $PtSn_x$ NPs are fairly uniformly distributed over the surface of the tin-containing phase. It is likely that this phase is a mixture of crystalline tin dioxide and amorphous tin hydroxides and sodium stannates, which were formed in the course of electrolyte preparation.

The electrocatalytic activity[¶] of the catalysts was studied in the ethanol electrooxidation reaction (EOR) in acidic media. Figure 4(*a*) shows a typical cyclic voltammogram (CV) measured in a 0.5 M H_2SO_4 + 2.0 M EtOH electrolyte on a Pt-based catalyst. In the anodic scan, a peak at ~0.5–1.0 V corresponds to the oxidation of ethanol molecules adsorbed on the $PtSn_x$ or Pt surfaces. A further decrease in the current density can be attributed

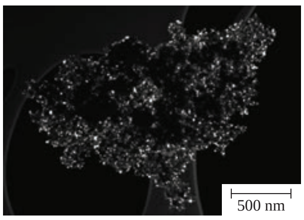

Figure 3 STEM image of the $PtSn_x$ sample.

[§] The STEM measurements were made on a JEOL JEM 1400 microscope at an accelerating voltage of 120 kV in the light field. Samples were prepared by dispersion in ethanol and exposed to ultrasound for 10 min. A droplet with suspended particles was applied onto copper meshes covered with a carbon film (Holey Carbon Grid).

[¶] The 'catalytic ink' contained the Pt/C or $PtSn_x$/C catalysts and a 10% Nafion® DE-1020 solution. Electrochemical cycling performance tests were implemented in a three-electrode cell in 0.5 M H_2SO_4 containing EtOH (0.25, 0.50, 1.0, and 2.0 mol dm^{-3}) deaerated with N_2 over a potential range of 0.05–1.5 V.

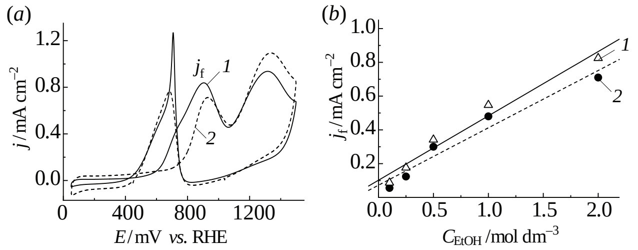

Figure 4 (*a*) CV curves of (*1*) $PtSn_x$/C and (*2*) Pt/C electrocatalysts in a 0.5 M H_2SO_4 + 2.0 M EtOH solution, scan rate 50 mV s^{-1}; (*b*) dependence of j_f on ethanol concentration for (*1*) $PtSn_x$/C and (*2*) Pt/C.

to a decrease in the coverage degree for the adsorbed ethanol molecules on the metal surface and the coverage (at $E > 1.0$ V) of the adsorption centers with oxygen molecules. During the cathodic scan, a similar peak due to ethanol oxidation was also observed.

Tin or tin oxides are good promoters for EOR on Pt-based catalysts.[21,30] According to Figure 4(*a*), the rate of EOR on the $PtSn_x$/C electrocatalyst is higher than that on Pt/C by a factor of 1.5. In addition, the onset potential for EOR on $PtSn_x$/C is almost 200 mV lower than that on Pt/C. This can be due to the fact that the EOR on tin-containing catalysts occurs according to the bifunctional mechanism:

$$Pt + CO \rightarrow Pt\text{–}CO_{ad}, \qquad (1)$$

$$Sn + H_2O \rightarrow Sn\text{–}OH_{ad} + H^+ + e^-, \qquad (2)$$

$$Pt\text{–}CO_{ad} + Sn\text{–}OH_{ad} \rightarrow CO_2 + H^+ + e^-. \qquad (3)$$

Note that the peak current density j_f in the forward scan of the CV curve increased linearly with the ethanol concentration [Figure 4(*b*)]. Thus, the electrooxidation of ethanol on both Pt/C and $PtSn_x$/C is limited only by the diffusion of ethanol molecules onto the electrode surface.

In conclusion, we prepared the tin-doped Pt nanoparticles by a modified EDPAC technique. The presence of tin ions in alkaline electrolyte has almost no effect on the rate of platinum dispersion (V_{disp}). According to the XRD data, the size of $PtSn_x$ nanoparticles averaged over all crystallographic directions was 5.6 nm. A tin oxide phase was identified in the synthesized material. The $PtSn_x$ nanoparticles were supported onto carbon black surface, and their electrocatalytic activity towards ethanol electrooxidation was investigated. The catalytic activity of the tin-doped Pt-based catalyst in ethanol electrooxidation was better than that of Pt/C electrocatalysts obtained using a similar approach. The rate of ethanol oxidation on the $PtSn_x$/C electrocatalyst was ~1.5 times higher than that on Pt/C. Moreover, the onset potential on the former was almost 200 mV lower than that on the latter. The results indicate that EDPAC can be efficiently applied to the preparation of catalysts based on tin-doped platinum nanoparticles.

The XRD and TEM measurements were carried out with financial support of the Russian Foundation for Basic Research (project no. 18-33-20064 mol_a_ved). All electrochemical measurements were performed within the framework of the Grant of the President of the Russian Federation for young PhD scientists (project no. MK-194.2019.3).

References

1 C. Baldizzone, S. Mezzavilla, H. W. P. Carvalho, J. C. Meier, A. K. Schuppert, M. Heggen, C. Galeano, J.-D. Grunwaldt, F. Schüth and K. J. Mayrhofer, *Angew. Chem., Int. Ed.*, 2014, **53**, 14250.

2 H. You, S. Yang, B. Ding and H. Yang, *Chem. Soc. Rev.*, 2013, **42**, 2880.

3 G. Hu, F. Nitze, E. Gracia-Espino, J. Ma, H. R. Barzegar, T. Sharifi, X. Jia, A. Shchukarev, L. Lu and C. Ma, *Nature Commun.*, 2014, **5**, 1.

4 V. R. Stamenkovic, B. S. Mun, M. Arenz, K. J. Mayrhofer, C. A. Lucas, G. Wang, P. N. Ross and N. M. Markovic, *Nat. Mater.*, 2007, **6**, 241.
5 Y.-J. Wang, N. Zhao, B. Fang, H. Li, X. T. Bi and H. Wang, *Chem. Rev.*, 2015, **115**, 3433.
6 M. N. Obrovac and V. L. Chevrier, *Chem. Rev.*, 2014, **114**, 11444.
7 K. Maeda, K. Teramura, H. Masuda, T. Takata, N. Saito, Y. Inoue and K. Domen, *J. Phys. Chem. B*, 2006, **110**, 13107.
8 Q. Meng and Z. Yin, *Mendeleev Commun.*, 2019, **29**, 672.
9 Z. Chen, B. Ge, W. Li, S. Lin, J. Shen, Y. Chang, R. Hanus, G. J. Snyder and Y. Pei, *Nat. Commun.*, 2017, **8**, 13828.
10 B. Hamdou, J. Gooth, T. Böhnert, A. Dorn, L. Akinsinde, E. Pippel, R. Zierold and K. Nielsch, *Adv. Energy Mater.*, 2015, **5**, 1500280.
11 C. Cui, L. Gan, M. Heggen, S. Rudi and P. Strasser, *Nat. Mater.*, 2013, **12**, 765.
12 H.-H. Li, C.-H. Cui, S. Zhao, H.-B. Yao, M.-R. Gao, F.-J. Fan and S.-H. Yu, *Adv. Energy Mater.*, 2012, **2**, 1182.
13 K. Hagedorn, B. Liu and A. Marcinkevicius, *J. Electrochem. Soc.*, 2012, **160**, F106.
14 Z. Swiatkowska-Warkocka, A. Pyatenko, F. Krok, B. R. Jany and M. Marszalek, *Sci. Rep.*, 2015, **5**, 9849.
15 B. Grushko, *J. Alloys Compd.*, 2019, **792**, 1223.
16 N. Jain, A. Roy and S. Nair, *Nanoscale*, 2019, **11**, 22423.
17 V. V. Yanilkin, N. V. Nastapova, R. R. Fazleeva, G. R. Nasretdinova, E. D. Sultanova, A. Yu. Ziganshina, A. T. Gubaidullin, A. I. Samigullina, V. G. Evtugin, V. V. Vorobev and Yu. N. Osin, *Russ. Chem. Bull., Int. Ed*., 2018, **67**, 215 (*Izv. Akad. Nauk, Ser. Khim*., 2018, 215).
18 V. V. Yanilkin, R. N. Gul'naz and V. A. Kokorekin, *Russ. Chem. Rev.*, 2018, **87**, 1080.
19 A. F. B. Barbosa, V. Del Colle, N. A. Galiote and G. Tremiliosi-Filho, *J. Electroanal. Chem.*, 2020, **857**, 113734.
20 P. Chandran, D. Puthusseri and S. Ramaprabhu, *Int. J. Hydrogen Energy*, 2019, **44**, 4951.
21 A. B. Kuriganova and N. V. Smirnova, *Mendeleev Commun.*, 2014, **24**, 351.
22 Y. Li, C. Liu, Y. Liu, B. Feng, L. Li, H. Pan, W. Kellogg, D. Higgins and G. Wu, *J. Power Sources*, 2015, **286**, 354.
23 Y. Gu, C. Liu, Y. Li, X. Sui, K. Wang and Z. Wang, *J. Power Sources*, 2014, **265**, 335.
24 Q. Wang, G. Wang, H. Xin, J. Liu, G. Xiong, P. Wu and X. Li, *Catal. Sci. Technol.*, 2019, **9**, 3226.
25 A. B. Kuriganova, I. N. Leontyev, O. A. Maslova and N. V. Smirnova, *Mendeleev Commun.*, 2018, **28**, 444.
26 N. V. Smirnova, A. B. Kuriganova, D. V. Leont'eva, I. N. Leont'ev and A. S. Mikheikin, *Kinet. Catal.*, 2013, **54**, 255 (*Kinet. Katal.*, 2013, **54**, 265).
27 A. B. Kuriganova, I. N. Leont'ev and N. V. Smirnova, *Russ. J. Electrochem.*, 2018, **54**, 561 (*Elektrokhimiya*, 2018, **54**, 646).
28 A. A. Ulyankina, A. B. Kuriganova and N. V. Smirnova, *Mendeleev Commun.*, 2019, **29**, 215.
29 I. N. Leontyev, A. B. Kuriganova, N. G. Leontyev, L. Hennet, A. Rakhmatullin, N. V. Smirnova and V. Dmitriev, *RSC Adv.*, 2014, **4**, 35959.
30 N. S. Marinkovic, M. Li and R. R. Adzic, in *Electrocatalysis*, ed. M. Shao, Springer International Publishing, Cham, 2020, pp. 1–39.

Received: 21st April 2020; Com. 19/6203